Real-time imaging of atomistic process in one-atom-thick metal junctions

V. Rodrigues[1,2] and D. Ugarte[1,*]
[1]*Laboratório Nacional de Luz Síncrotron, Caixa Postal 6192, 13084-971 Campinas SP, Brazil*
[2]*Intituto de Física Gleb Wathagin, UNICAMP, Caixa Postal 6161, 13083-970 Campinas SP, Brazil*
(Received 14 August 2000; published 26 January 2001)

We present an *in situ* and time resolved high-resolution transmission electron microscopy study of the atomistic process during the last elongation stages of gold nanojunctions. In particular, we concentrate on suspended chains of atoms, which have shown to be remarkably stable, although they present rather long bonds (3.0–3.6 Å). One-atom-thick junctions are robust, but their attachment points move rather easily on the metal surface, allowing the accommodation of apex movements or rotations.

DOI: 10.1103/PhysRevB.63.073405 PACS number(s): 68.65.−k, 68.37.Lp, 61.46.+w

The understanding of the mechanical properties of nanometric junctions has enormous interest in many different scientific and technological domains such as nanoelectronics, wear, adhesion, friction, etc.[1] Recently, the quantized electrical conductance properties of nanowires[2] has sparked an intense research activity on the elongation of metallic contacts, because the stretching and further rupture of nanojunctions (NJs) represents the basic experiment to generate atom size conductors.[3–5]

The NJ elongation shows alternating stages of elastic deformation and yielding,[1,6] and in order to understand the structural evolution, it is necessary to analyze the underlying mechanisms and their kinetics. Most of the available information on this topic has been obtained from large scale molecular dynamics simulations,[1,3,7–12] which have the advantage of being able to look at the atomic positions and see how they change in situations that may be extremely difficult to obtain experimentally. However, any atomistic simulation is actually a function of the atomic interaction (or interatomic potential), and the accuracy of the predictions is often tricky to estimate because of the difficulty of performing a comparison with experimental data.

Because experimental information on NJ structure evolution is rather limited,[13–15] dynamic experiments involving the real-time observation of a microscopic process attract enormous interest, and are fundamental to developing a new understanding of the physical phenomena. In this sense, high-resolution transmission electron microscopy (HRTEM) is a very powerful technique because it allows the combination of atomic resolution with real-time image acquisition [time resolution is usually limited to television (TV) rate 1/30 s]. Using a TEM sample holder including a simplified scanning tunnel microscope (STM), Ohnishi *et al.*[15] have provided direct evidence of the generation of linear gold atom chains (ATC) for NJ under tensile stress.[12,16] These authors also generated ATC by elongating nanobridges generated from a continuous gold film,[17] and were able to measure unexpected interatomic bond lengths as long as 3.6 Å.[15,16]

In this paper, we present a time-resolved HRTEM study of the elongation of gold NJs, in particular, we analyze both the atomic structure and also the dynamic processes involved in the formation and evolution of one-atom-thick junctions. We must keep in mind that we will be imaging the movements of a strand formed by single atoms, which represents a quite stringent observation from the point of view of electron microscopy methods. We anticipate that these results will be very important in understanding the atomistic mechanism involved in the elongation and rupture of atom size junctions, and also to develop novel theoretical descriptions capable of simulating physical microscopic mechanisms with better accuracy.

Gold NJ's were generated *in situ* in a HRTEM (JEM 3010 UHR 300 kV LaB_6 gun, 0.17 nm resolution, LME/LNLS Campinas, Brazil) following the procedure proposed by the work of Takayanagi's group.[15,17] Neighboring holes are perforated in a polycrystalline gold thin film using a focused electron beam (current density 100 A/cm^2); further irradiation induces the diameter of the holes to grow until a nanometric bridge is formed. At this point, the electron-beam current density is reduced to more usual values (~30 A/cm^2) for image recording. The generated metal necks showed a tendency to elongate, become thinner, and finally break (this process usually took 5–30 min). This stretching process is attributed to a general deformation of the whole thin film that generates clearly noticeable relative displacement of the NJ apexes.[18] The sample temperature during observations could not be monitored, but it can be roughly estimated to be around room temperature.[14] HRTEM micrographs were acquired using a digital camera (Gatan MSC794, acquisition time ~1 s) and real-time evolution was recorded using a high sensitivity TV camera (Gatan 622SC, 30 frame/s) associated with a conventional video recorder. The subsequent digitization of the video tape limited the time resolution to ~0.085 s per frame. Most of the images shown in this work have been obtained by adding 5–6 digitized frames to improve the signal-to-noise ratio. It must be emphasized that the intense electron irradiation, necessary to make holes in the film, is also helpful to get clean gold nanostructures, because it transforms amorphous-C contamination (if present) into spherical multishell fullerenes (bucky-onions).[19]

Figure 1 shows some snapshots of a whole NJ rupture process; the first shows an elongated rodlike morphology and some (200) gold planes ($d_{200}=2.05$ Å) can be seen on the lower apex. Some instants later, a one-atom-thick junction is generated [Fig. 1(b) ATC length ~10 Å] where the atomic positions (black dots) can be easily identified (interatomic distance 3.2 ± 0.2 Å); note the important clockwise rotation

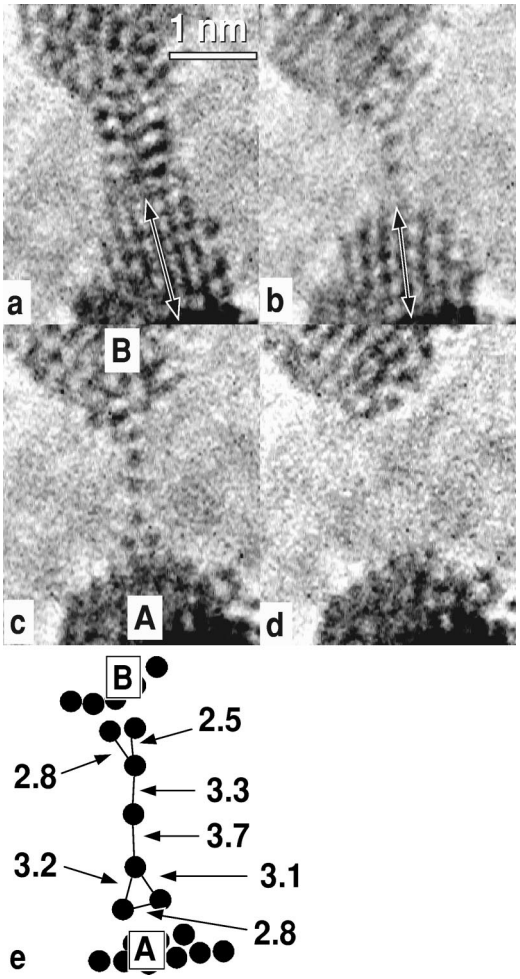

FIG. 1. Time sequence of atomic resolution images of the formation, elongation and fracture of a suspended chain of gold atoms: (a) 0 s; (b) 0.64 s; (c) 1.12 s; and (d) 3.72 s. Atomic positions appear as dark lines or dots. A schematic representation of the chain structure is shown in (e) (distances are marked in Å and the error bar is 0.1 Å); the letters A and B indicate the apex position in (c). Note that the chain is attached to the tips through a two atom structure. The double arrows in (a) and (b) have been drawn to indicate the movement (rotation) of the lower apex.

(~8°) of the lower apex atomic planes (marked with double arrows in Fig. 1). The apex rotation indicates that although the atom chain is strong enough to hold the junction together, it absorbs bending efforts and allows apex movements. The apexes display sharp tips to which the chain seems to be strongly bound. An additional ~9 Å junction elongation induces the incorporation of more atoms into the chain that becomes formed by three suspended atoms that are fixed to the apex tips through two atom connections [Fig. 1(c)]. We must note that the atom separation in the chain is bigger than that in the sticking sites [see schematic drawing in Fig. 1(e)]. Finally, the atomic chain breaks, and the apexes separate by an additional ~5 Å. The apex rotation and the increase of their separation during the rupture process confirm that the structural evolution can be mainly attributed to strain.

In many atom chain images the atomic positions cannot always be resolved, the main factor responsible for this difficulty is the fact that these structures are rather mobile (at least for the time resolution in our experiments): the sticking position on the apex surface changes frequently during elongation. This behavior is displayed in Fig. 2, where we show the atom chain elongation dynamics, and in particular, its movements (the chain is indicated by white arrows on the apexes). Initially, the junction has a biconical shape, and the minimal constriction is about 10 Å in diameter [Fig. 2(a)]. In Fig. 2(b), the constriction is formed by a single gold atom hanging between the apexes; the suspended atom is located equidistant from the tips (i.e., bond length of 3.1 ± 0.2 Å). In Fig. 2(c), the chain shows an additional elongation (intertip separation is 9.0 ± 0.2 Å) but unfortunately the atomic positions cannot be resolved; the lower apex is sliding towards the right and the chain shows an ~18° inclination angle. Some instants later [Fig. 2(d)], the lower ATC attachment point has glided towards the left along the lower apex [111] facet and recovered the vertical orientation. At this moment, the junction is slightly longer (9.6 ± 0.2 Å) and the ATC is formed by three atoms separated by 3.2 ± 0.2 Å. Subsequently, the chain stretches to attain 12.6 ± 0.2 Å, apparently by the inclusion of an additional atom, but atomic positions cannot be resolved [Fig. 2(e)]. On the left facet of the upper apex, an atomic terrace is indicated by a black arrow in Fig. 2(e), later, the upper ATC sticking point moves to this atomic step [Fig. 2(f)]. The apex separation has become 13.6 ± 0.2 Å and, the lower ATC extreme has become fixed to the sharp tip of a well-defined pyramidal apex. Finally, the chain breaks apart (not shown). The preceding image sequence shows both the chain elongation and also how the apex movements are easily accommodated by a flexible chain attachment to the surface and through the chain diffusion on the apex surface. We must remark that the chain is strongly bound to the tips, inducing the formation of well-faceted sharp pyramids [see Fig. 2(e)] but the ATC extreme seems to move rather easily on the metal surface. This be-

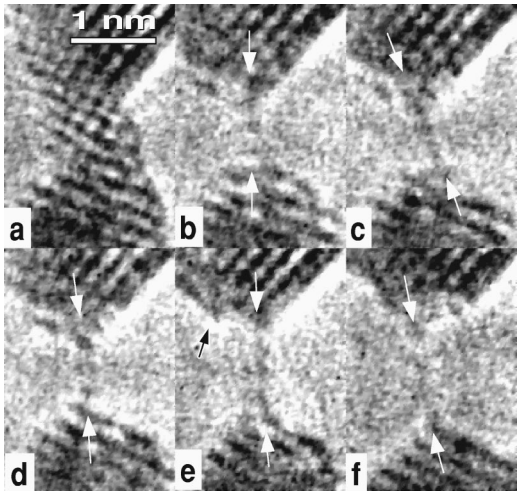

FIG. 2. Sequence of images showing the movements of a gold atomic chain subjected to a slow mechanical stretching. (a) 0 s, (b) 10 s, (c) 64 s, (d) 66 s, (e) 75 s, and (f) 85 s, respectively. Atomic positions appear as dark lines or dots. Note that this ATC display a remarkable long lifetime ($>$ 1 min.) and moves on the apex surfaces.

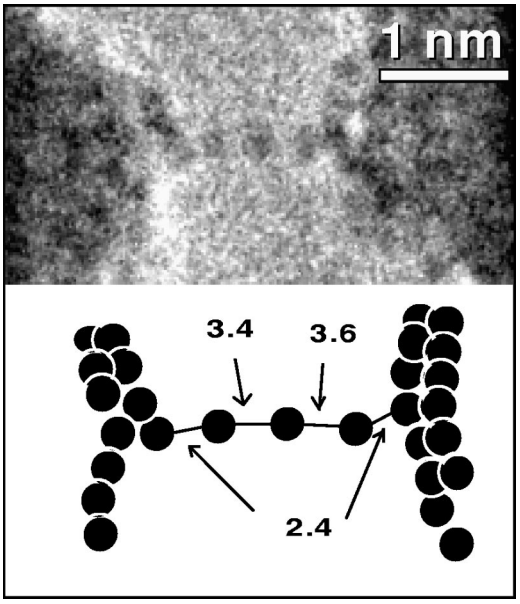

FIG. 3. HRTEM image of an atom chain formed by three gold atoms (upper part). Atomic positions appear as dark dots. A schematic representation is shown at the lower part (distances are marked in Å). Note that the distances between the apexes and the suspended atoms are shorter than inside the chain.

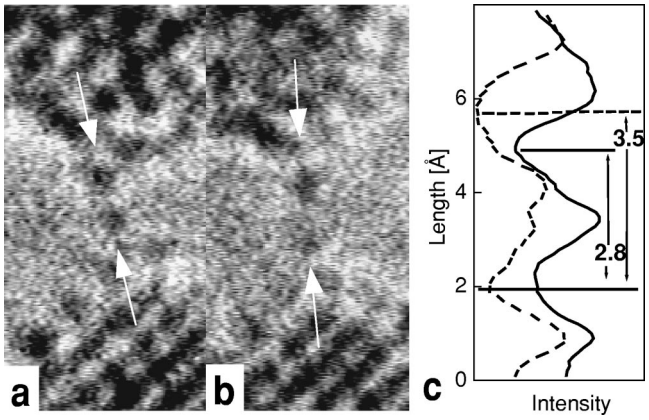

FIG. 4. Time sequence of the elongation of an ATC formed by two atoms (atomic positions appear as dark dots): (a) 0 s; (b) 3.2 s. At the right, we show the intensity profiles along the ATC in (a) and (b) (profiles directions indicated with arrows); bond lengths between the suspended atoms (intensity minima) are indicated in Å.

havior is analogous to gold atoms, for example, on compact surfaces, which show a rather low diffusion barrier ($\sim$0.1 eV)[20] when compared to the cohesion energy for bulk atoms ($\sim$3.8 eV) or surfaces atoms ($\sim$1 eV).[6]

Images presented in Figs. 1 and 2 were obtained by digitizing video recordings; but sometimes ATCs stayed static on a fixed position for many seconds, allowing the acquisition of high quality micrographs as shown in Fig. 3. We can note that the inter-atomic distance is not regular along the structure: the central atom is approximately equidistant from the other two (3.4 and 3.6 ± 0.1 Å, while the tip-suspended atom distances are smaller (2.4 ± 0.1 Å). This bond-length distribution is the usual pattern in our observations [see also Figs. 1(c), 2(d), and 4(b)]. Additional important insights can be obtained by looking carefully at the evolution of ATC bond lengths under a tensile deformation. Figure 4 shows the effect of an interapex distance increase ($\sim$1.5 Å) on an ATC formed by two atoms. The significant elongation of the bond between the suspended atoms (from 2.8 to 3.5 ± 0.2 Å) indicates that this region absorbs most of the linear deformation, while the sticking ATC bonds stay shorter.

At this point, it is worthwhile to discuss the bonding of gold atoms in an ATC structure, which represents a subject still not fully resolved. For example, although the nearest-neighbor distance in macroscopic gold is $\sim$2.88 Å, our results, as well as prior experiments,[15,16] point to rather long interatomic distances (3.4–3.6 Å). Although these bonds may seem to be rather long, the structure may last many seconds, even in the harsh environment of a TEM.

Metallic bonding is generated by electron delocalization, and it is mostly non-directional; this allows metal atoms to slide past each other more easily than in directional bonding types (such as covalent). These effects are particularly pronounced for gold and they induce that the surface and volume atoms can easily reorganize and minimize the total energy of a nanostructure.[21] These facts explain the reported apex morphology and nanowire structures,[18] but the long interatomic bond lengths (>3 Å) in gold ATC cannot be easily understood. Actually, these long bonds represent a challenge for theoretical calculations performed using different approaches,[12,22–24] which predict that stable ATCs can only be obtained with shorter interatomic distances (2.4–2.9 Å). Also, a dimerization of the chain atoms has been suggested[22] in contrast with the experimentally observed bond-length distribution (Fig. 3). From a rather different perspective, a rotating zizzag ATC geometry has recently been proposed to explain the long bond lengths observed in HRTEM images.[23] However, our results do not support this model, because the rotation of a high atomic number atom, such as gold, would generate ghost dots, which would be easily detected considering the signal-to-noise ratio of our HRTEM images.

Regardless of the bond length, the strength of the atom size junction has been measured to be 10–20 times higher than macroscopic gold[6,25] and this effect has been associated with the difficult generation of extended defects in these small structures.[26] From the point of view of cohesion, several calculations indicate that quantization of transverse electron motion induces the generation of subbands (or conduction channels) that act as delocalized chemical bonds.[23,27] In fact, the contribution of these electronic states to the binding energy[27] accounts for almost the total force fluctuation measured experimentally in atomic size NJs.[6,25] Surprisingly, a similar conclusion was obtained for the proposed zigzag atomic wire, where the structure stabilization was attributed to delocalized electrons instead of chemical-bond directionality.[23]

In view of these facts, the remarkable stability of ATC in the HRTEM must be carefully analyzed from other points of view, as for example, possible charging effects due to the interaction with the electron beam.[24] The existence of gold ATCs was revealed using a ultrahigh vacuum ($\sim 10^{-10}$ Torr) TEM equipped with a field-emission gun

where the electron current was ~ 0.05 A/cm^2.[15] Two different *in situ* HRTEM methods were used for the junction generation by Ohnishi *et al.*,[15] the first one produced a NJ between a fixed electrode and a mobile STM tip, but the imaging of individual atoms composing the ATC was not possible. In contrast, the second approach, also used in this work, has allowed the measurement of the long interatomic bond lengths, because NJs form a monolithic structure where apexes and the NJs were part of a continuous gold film. In addition, this structure guarantees the perfect grounding of both apexes (NJ leads) considering that the electron beam homogeneously illuminated the whole area of interest. It must be emphasized that our measurements were performed using different experimental conditions, where the vacuum quality is lower ($\sim 10^{-7}$ Torr) and the current was about six hundred times higher. However, the results are indeed quite similar, both concerning the interatomic distances and the most frequently observed ATC lengths (3–4 atoms), demonstrating the validity of the derived ATC structural parameters.

We must remark that most of the information of atomistic process in a mechanically deformed NJ has been previously obtained by means of molecular dynamics simulations where the typical elongation speed (a few meters/s[1,3,7–12]) is several order of magnitude (10^8–10^9) faster than in normal STM experiments ($\sim$nm/s).[3,6,7,25] The evolution of atom chains displayed in this study was obtained with an average elongation speed of ~ 0.1 nm/s, actually very close to the NJ force or conductance experiments, confirming the importance of real-time HRTEM experiments to study microscopic mechanisms in NJs.

In summary, we have been able to experimentally observe the atomistic process involved during the last elongation steps of gold NJs and get direct real-space information on atomic positions, bond lengths, and also how they change during a rupture process. The suspended ATCs are remarkably stable and display extremely long interatomic distances (3.0–3.6 Å), in agreement with a previous report.[15] One-atom-thick NJs are robust, but their attachment points on a metal surface are capable of moving rather easily. These are fundamental inputs for testing new theoretical tools (such as potentials) to be used in numerical simulations of atomistic processes in materials. The mobility of the ATC fixing points may have important effects, for example, it may change the atomic wire-apex electronic coupling[28] and generate small variations (substructures) in the quantum conductance response.[29]

We thank the LNLS, CNPq, and FAPESP (Contract Nos. 1996/12546-0 and 1998/13501-6) for financial support.

*Email address: Author to whom correspondence should be addressed: ugarte@lnls.br

[1] U. Landman, W. D. Luedtke, N. A. Burnham, and R. J. Colton, Science **248**, 454 (1990).
[2] H. van Houten and C. Beenakker, Phys. Today **49**, 22 (1996).
[3] L. Olesen, E. Lægsgaard, I. Stensgaard, F. Besenbacher, J. Schiøtz, P. Stoltze, K. W. Jacobsen, and J. K. Nørskov, Phys. Rev. Lett. **72**, 2251 (1994).
[4] J. M. Krans, J. M. van Ruintenbeek, V. V. Fisun, I. K. Yanson, and L. J. de Jongh, Nature (London) **375**, 767 (1995).
[5] J. L. Costa-Krämer, N. García, P. García-Mochales, and P. A. Serena, Surf. Sci. **342**, L1144 (1995).
[6] G. Rubio, N. Agraït, and S. Vieira, Phys. Rev. Lett. **76**, 2302 (1996).
[7] J. I. Pascual, J. Méndez, J. Gómes-Herrero, A. M. Baró, N. Garcia, U. Landman, W. D. Luedtke, E. N. Bogachek, and H.-P. Cheng, Science **267**, 1793 (1995).
[8] M. Brandbyge, J. Schiøtz, M. R. Sørensen, P. Stoltze, K. W. Jacobsen, J. K. Nørskov, L. Olesen, E. Lægsgaard, I. Stensgaard, and F. Besenbacher, Phys. Rev. B **52**, 8499 (1995).
[9] T. N. Todorov and A. P. Sutton, Phys. Rev. Lett. **70**, 2138 (1993).
[10] A. M. Bratkovsky, A. P. Sutton, and T. N. Todorov, Phys. Rev. B **52**, 5036 (1995).
[11] U. Landman, W. D. Luedtke, B. E. Salisbury, and R. L. Whetten, Phys. Rev. Lett. **77**, 1362 (1996).
[12] M. R. Sørensen, M. Brandbyge, and K. W. Jacobsen, Phys. Rev. B **57**, 3283 (1998).
[13] T. Kizuka, Phys. Rev. B **57**, 11 158 (1998).
[14] T. Kizuka, Phys. Rev. Lett. **81**, 4448 (1998).
[15] H. Ohnishi, Y. Kondo, and K. Takayanagi, Nature (London) **395**, 780 (1998).
[16] A. I. Yanson, G. Rubio Bollinger, H. E. van den Brom, N. Agraït, and J. M. van Ruintenbeek, Nature (London) **395**, 783 (1998).
[17] Y. Kondo and K. Takayanagi, Phys. Rev. Lett. **79**, 3455 (1997).
[18] V. Rodrigues, T. Furher, and D. Ugarte, Phys. Rev. Lett. **85**, 4124 (2000).
[19] D. Ugarte, Nature (London) **359**, 707 (1992); see also D. Ugarte, Chem. Phys. Lett. **209**, 99 (1993).
[20] A. Pimpinelli, J. Villain, and C. Godreche, *Physics of Crystal Growth* (Cambridge University, Cambridge, England, 1998), pp. 121.
[21] L. D. Marks, Rep. Prog. Phys. **57**, 603 (1994).
[22] H. Häkkinen, R. N. Barnett, and U. Landman, J. Phys. Chem. B **103**, 8814 (1999).
[23] D. Sánchez-Portal, E. Artacho, J. Junquera, P. Ordejón, A. García, and J. M. Soler, Phys. Rev. Lett. **83**, 3884 (1999).
[24] J. A. Torres, E. Tosatti, A. Dal Corso, F. Ercolessi, J. J. Kohanoff, F. D. Di Tolla, and J. M. Soler, Surf. Sci. **426**, L441 (1999).
[25] S. P. Jarvis, M. A. Lantz, H. Ogiso, H. Tokumoto, and U. Dürig, Appl. Phys. Lett. **75**, 3132 (1999).
[26] U. Durig, in *Nanowires*, Vol. 340 of *NATO Advanced Studies Institute Series*, edited by P. A. Serena and N. García (Kluwer, Dordrecht, 1997), pp. 275.
[27] C. A. Stafford, D. Baeriswyl, and J. Burki, Phys. Rev. Lett. **79**, 2863 (1997); J. M. van Ruitenbeek, M. H. Devoret, D. Esteve, and C. Urbina, Phys. Rev. B **56**, 12 566 (1997); S. Blom, H. Olin, J. L. Costa-Krämer, N. García, M. Jonson, P. A. Serena, and R. I. Shekhter, *ibid.* **57**, 8830 (1998).
[28] A. Levy Yeyati, A. Martín-Rodero, and F. Flores, Phys. Rev. B **56**, 10 369 (1997).
[29] W. A. de Heer, S. Frank, and D. Ugarte, Z. Phys. B: Condens. Matter **104**, 469 (1997).